Macromolecules
ARTICLE

Macromolecules **2009**, *42*, 6141–6146 **6141**
DOI: 10.1021/ma9011208

Novel and Accurate Method for Determination of Glass Transition Temperature of Spin-Labeled Polymer by ESR Microwave Power Saturation

Yohei Miwa*,†

Department of Chemistry and Biochemistry, University of Detroit Mercy, 4001 West McNichols Road, Detroit, Michigan 48221-3038. †Present address: Mitsubishi Chemical Group Science and Technology Research Center, Inc., Japan.

Received May 22, 2009; Revised Manuscript Received July 2, 2009

ABSTRACT: A novel method to determine a glass transition temperature (T_g) of spin-labeled polymer applying the continuous-wave electron spin resonance (CW-ESR) has been developed. Poly(cyclohexyl acrylate) (PCHA), polystyrene (PS), poly(methyl acrylate) (PMA), poly(propylene glycol) (PPG), and poly(ethylene glycol) (PEG) were labeled by attachment of nitroxide radicals; the temperature-dependent microwave power saturation measurements were carried out. The saturation factor, S, determined from the microwave power saturation measurement, had different temperature dependence above and below the T_g of the spin-labeled polymer because of the different temperature dependence of the spin−lattice relaxation time. The inflection point in the temperature dependence of S was defined as a $T_{g,\ ESR}$. The $T_{g,\ ESR}$ was in good agreement with the $T_{g,\ DSC}$ determined by differential scanning calorimetry (DSC) for the PCHA, PS, PMA, and PPG. The $T_{g,\ ESR}$ of the PCHA labeled at the chain end was about 3 K lower than that of the one labeled at the midchain segments, which indicated that the local T_g around chain ends is slightly depressed. Furthermore, the $T_{g,\ ESR}$ of highly crystallized PEG was determined to 221 K even though the DSC was unable to detect the glass transition. This value agreed well with the T_g of PEG determined by thermally stimulated current.

Introduction

A glass transition is one of the most important physical phenomena for polymeric materials; therefore, many methods, for example differential scanning calorimetry (DSC), dilatometry, dynamic mechanical analysis, etc., have been applied to determine a glass transition temperature (T_g).[1] On the other hand, recent interest is directed toward the determination of local T_g's in polymeric materials, such as polymer/inorganic filler interface, immiscible polymer/polymer interface, and free surface of polymer films because local physical properties are scientifically interesting and practically important for applications of the materials.[2] However, selective determination of local T_g's is hard by the conventional methods. Recently, Ellison and Torkelson developed a new T_g measurement technique using fluorescence measurements.[3] This method is unique because local T_g around fluorescence labels can be determined selectively. They prepared multilayer films of labeled and unlabeled polystyrene and successfully showed that there is a large difference in T_g between the regions near the free surface and those near the substrate. Label methods are effective to determine the local T_g selectively.

The fluorescence label technique is one of the excellent label techniques to detect local T_g's in polymeric materials. However, determination of the T_g of polymers which are confined in opaque solids such as a polymer thin film sandwiched by metal or inorganic plates is hard by the fluorescence method because the detection of the fluorescence from the sample is difficult. On the other hand, electron spin resonance (ESR) detects a signal using a microwave. Therefore, the ESR based on the spin-label technique is useful to discern different sites in complex systems even for opaque systems. In this technique, the mobility of the labels is usually determined by the spectral simulation with proper algorithms accounting for the stochastic nature of the molecular motion.[4] For the X-band ESR spectroscopy, the spectral shape is sensitively changed by the label motion on time scales in the range $10^{-11}-10^{-7}$ s.[5] However, the determination of a T_g is hard by this method because the change of the ESR spectral shape is little at the T_g of the spin-labeled polymer. On the other hand, some advanced ESR techniques were applied to detect the change of spin−lattice relaxation time, T_1, at the glass transition. Andreozzi et al. determined the temperature dependent T_1 of poly((4-pentiloxy-3′-methyl-4′-(6-acryloxyexyloxy))azobenzene) containing small amount of the cholestane probe by longitudinally detected ESR (LODESR).[6] They found that the temperature dependence of the T_1 around the T_g is described well by a law of the William−Landel−Ferry (WLF) form. This result shows that there is a correlation between the T_1 and the viscosity of amorphous materials around the T_g. Sato et al. determined temperature dependent T_1 of glass-forming solvents (decalin, glycerol, 3-methylpentane, *o*-terphenyl, 1-propanol, sorbitol, sucrose, octaacetane, and 1:1 water:glycerol) containing small amount of nitroxides by long-pulse saturation recovery technique.[7] Different temperature dependences of the T_1^{-1} were observed above and below the T_g of the glass-forming solvents because the rates of molecular tumbling increased as the glass matrix softened. Spielberg and Gelerinter studied the molecular dynamics of a nematic liquid crystal, *n*-(*p*-methoxybenzlidene)-*p*-butylaniline, using the conventional CW-ESR spin-probe technique.[8,9] They found sudden changes in ESR signal intensity at the glass transition, which is interpreted as resulting from ESR signal saturation effect associated with changes of the T_1.

*Corresponding author. Telephone and fax: +81-59-355-1350. E-mail: yo_hei38@hotmail.com.

Published on Web 07/14/2009

Table 1. Characteristics of Samples

notation	M_n	M_w/M_n	spin-label site	C_N (mol g^{-1})[a]	$T_{g,\ ESR}$ (K)	$T_{g,\ DSC}$ (K)
PCHA-1	14900	1.15	midchain	9.6×10^{-7}	287[b]	286
PCHA-2	14900	1.15	midchain	4.8×10^{-7}	285	286
PCHA-3	14900	1.15	midchain	1.3×10^{-7}	286	286
PCHA-E	15100	1.13	end	3.0×10^{-7}	284[c]	289
PCHA-P	14900	1.15	probe	5.0×10^{-7}	203	286
PS	5000	1.11	midchain	4.9×10^{-7}	360	356
PMA	28600	1.09	midchain	1.1×10^{-7}	285	281
PEG	4000		end	9.0×10^{-7}	221	218[d]
PPG	2000		end	8.1×10^{-7}	204	198

[a] Concentration of nitroxide. Determined by ESR. [b] Average of 286, 286, 287, and 289 K. [c] Average of 283, 284, and 286 K. [d] Determined by thermally stimulated current in ref 28.

In the present study, the T_g of spin-labeled polymers has been determined by the ESR microwave power saturation method. The T_g determined by the ESR technique, $T_{g,ESR}$, was in good agreement with that determined by the DSC, $T_{g,DSC}$, for the PCHA, PS, PMA, and PPG. This method was applied to determine the local T_g around the chain ends of the PCHA. Moreover, the $T_{g,\ ESR}$ of a highly crystallized PEG was determined while the DSC was unable to detect the glass transition of the PEG.

Experimental Section

Materials. Styrene (Extra Pure Reagent) and methyl acrylate (Extra Pure Reagent) were purchased from Nacalai Tesque Co., Ltd. Cyclohexyl acrylate (Extra Pure Reagent) was obtained from Kishida Chemical Co., Ltd. Poly(ethylene oxide) having a number-average molecular weight $M_n = 4000$ was purchased from Fluka Chemical Co., Ltd. *tert*-Butyl acrylate (Extra Pure Reagent), 2-bromopropionic acid *tert*-butyl ester (97%), and 1-phenylethyl bromide (95%) were purchased by Tokyo Chemical Co., Ltd. Poly(propylene glycol)bis(2-aminopropyl ether) ($M_n = 2000$), *N*,*N*,*N*′,*N*′,*N*″-pentamethyldiethylenetriamine (99%), methyl 2-bromo-propionate (98%), CuBr (98%), 1,1,4,7,10,10-hexamethyltriethylenetetramine (97%), anhydrous pyridine (99.8%), thionyl chloride (≥99%), 2,2,6,6-tetrametyl-4-aminopiperidine-1-oxyl (4-amino-TEMPO, 99%), 3-(carboxy)-2,2,5,5-tetramethyl-1-pyrrolidinyloxy (3-carboxy-PROXYL, 99%), 4-hydroxy-2,2,6,6-tetramethylpiperidine 1-oxyl (TEMPOL, 99%), and anhydrous diethyl ether (≥99.4%) were purchased from Aldrich and used as received. Benzene (≥99.5%, Aldrich) was dried with molecular sieves (8−12 Mesh, Beads Effective pore size 10 Å, Fisher Scientific Company) and calcium hydride (Eastman Kodak Company). Toluene, anisole, and methanol were obtained from Nacalai Tesque (Extra Pure Reagent) and used without further purification.

Spin-Labeling. Polystyrene (PS),[10] poly(methyl acrylate) (PMA),[11] and poly(cyclohexyl acrylate) (PCHA)[12] were polymerized by atom transfer radical polymerization (ATRP) and spin-labeled with 4-amino-TEMPO as described in our previous papers. The spin-labeling was carried out for midchain segments for the PS and PMA. On the other hand, for the PCHA, midchain segments or the chain ends were spin-labeled. The number averaged molecular weight (M_n) and the molecular weight distribution (M_w/M_n) were determined by the GPC with PS standards. Poly(ethylene glycol) (PEG) and poly(propylene glycol) (PPG) were spin-labeled with 3-carboxy-PROXYL at the chain ends. The spin-labeling of the PEG was described in our previous paper.[13] The PPG was spin-labeled by the same procedure with the PEG. The concentration of the nitroxide (C_N) in the samples was determined using a standard solution of TEMPOL in toluene as an intensity reference. The properties and notations of the samples are listed in Table 1. The chemical structures of the spin-labeled polymers are shown in Figure 1.

Spin-Probing. Nonlabeled PCHA and a small amount of TEMPOL were dissolved in toluene at 333 K, followed by solvent evaporation. The sample was then dried in a vacuum oven at 333 K for 6 h.

DSC Measurement. DSC measurement was carried out using Q10 differential scanning calorimeter manufactured by TA Instruments and calibrated with an indium standard. Cooling was accomplished by a TA Instruments quench cooler accessory. The DSC cell was purged with dry nitrogen flowing at a rate of 50 mL min^{-1}. Samples were heated from a room temperature to ca. $T_g + 50$ K at a rate of 20 K min^{-1}, kept for 5 min, and cooled at a rate of 10 K min^{-1}. The data collection was carried out on the cooling process. The $T_{g,\ DSC}$ was taken to be the midpoint, i.e., the temperature corresponding to half of the endothermic shift and included ±2 K of experimental uncertainties. The $T_{g,\ DSC}$ of the samples are listed in Table 1. Only for the PEG, the DSC measurement was carried out on the heating process from 163 to 383 K at the rate of 10 K min^{-1}.

ESR Measurement. ESR samples were contained into 3 mm o.d. quartz tubes and sealed under a vacuum. Spectra were recorded with JEOL X-band FA300 spectrometers with 100 kHz field modulation. The modulation amplitude was 0.2 mT. The temperature was controlled within ±0.1 K. All samples were allowed to equilibrate for at least 5 min after reaching the desired temperature. The temperature-dependent microwave power saturation measurement was carried out on the cooling process. The magnetic field and *g* tensor were calibrated with Mn^{2+}.

Gel Permeation Chromatography (GPC). GPC was carried out with following condition: in THF (1 mL/min) at 313 K on four polystyrene gel columns (Tosoh TSK gel GMH (beads size is 7 μm), G4000H, G2000H, and G1000H (5 μm)) that were connected to a Tosoh CCPE (Tosoh) pump and an ERC-7522 RI refractive index detector (ERMA Inc.). The columns were calibrated against standard PS (Tosoh) samples.

Results and Discussion

A. Determination of Glass Transition Temperature by ESR. Following the discussion of Brezina and Gelerinter,[14] the relative signal V_R from X-band ESR spectrometer is given by

$$V_R = \frac{\gamma H_1 (T_1 T_2)^{0.5}}{1 + \gamma^2 {H_1}^2 T_1 T_2} \quad (1)$$

where γ, H_1, T_1, and T_2 are the gyromagnetic ratio, microwave magnetic field, spin−lattice relaxation time, and spin−spin relaxation time, respectively. $\gamma^2 {H_1}^2 T_1 T_2$ is defined as a saturation factor, *S*, in this work. Below the saturation, V_R is proportional to H_1 because the *S* is small enough to be ignored. In experiments, V_R is usually plotted against the square root of the microwave power, $P^{0.5}$, because H_1 is proportional to $P^{0.5}$. The saturation curves of the PCHA-2 at 253 and 338 K are shown in Figure 2 where the V_R is obtained from a double integration of a spectrum. The V_R's normalized by the one measured at $P = 0.02$ mW, $V_R/V_{R,0.02mW}$, was proportional to $P^{0.5}$ when $P^{0.5}$ was small. On the other hand, the deviation from the linear relationship was observed with an increase in $P^{0.5}$ because of the microwave power saturation. The deviation demonstrates the increase in the *S*.

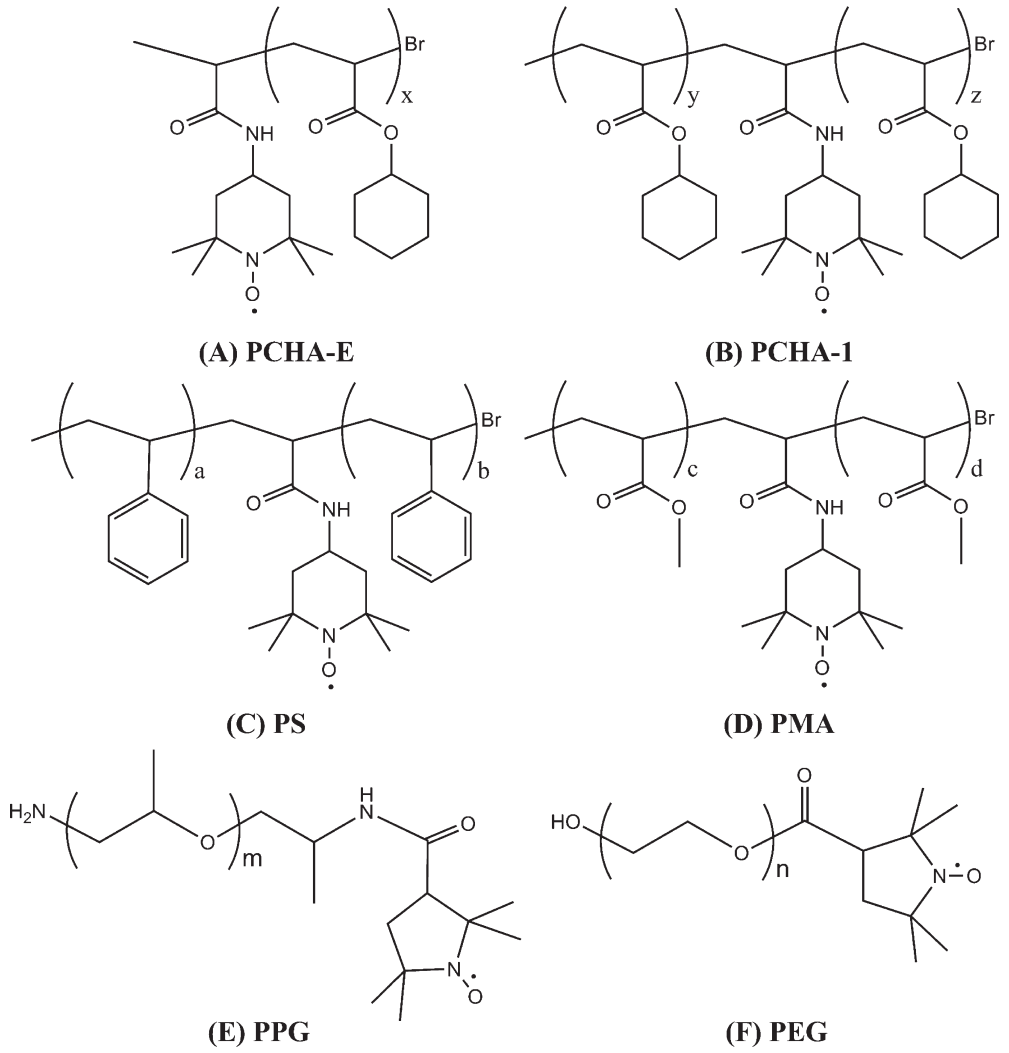

Figure 1. Chemical structures of PCHA-E (A), PCHA-1 (B), PS (C), PMA (D), PPG (E), and PEG (F).

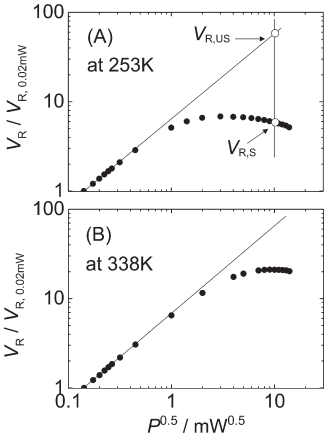

Figure 2. Plots of $V_R/V_{R,0.02mW}$ against $P^{0.5}$ for the PCHA-2 at 253 and 338 K. $V_{R,S}$ and $V_{R,US}$ are shown with arrows.

The S is determined from the saturation curve as follows: At the same $P^{0.5}$, the ratio of the V_R with saturation, $V_{R,S}$ to the one with unsaturation, $V_{R,US}$, is

$$\frac{V_{R,S}}{V_{R,US}} = \frac{1}{1+S} \tag{2}$$

Therefore, the S is given by

$$S = \frac{V_{R,US}}{V_{R,S}} - 1 \tag{3}$$

The schematic expression of the $V_{R,S}$ and $V_{R,US}$ is shown in Figure 2A.

The S determined at the P of 121 mW, S_{121mW}, for the PCHA-2 is plotted as a function of temperature in Figure 3. The temperature dependence of S_{121mW} showed an inflection at 285 K. This temperature is very close to the $T_{g,DSC}$, 286 K, of the PCHA-2. When the microwave power, P, is fixed, the S is a function of the T_1 and T_2. Therefore, the inflection demonstrates the change of the temperature dependences of the T_1 and T_2. The T_1 is proportional to the correlation time, τ_c, of molecular tumbling motion of nitroxides as the τ_c is longer than 10^{-7} s.[15] When nitroxides are attached to polymer chains, the mobility of nitroxides is strongly affected by that of polymer segments. Therefore, it is expected that the temperature dependence of the T_1 changes above and below the T_g because the temperature dependence of the polymer mobility dramatically changes around the T_g. In fact, the change of the temperature dependence of T_1 for cholestane probes dispersed in a polymer matrix at the polymer T_g was shown by the LODESR.[6] For various glass-forming solvents containing small amount of nitroxides, the different

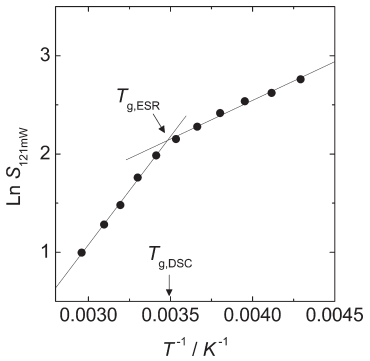

Figure 3. Temperature dependence of S_{121mW} for PCHA-2. The data points are least-squares fitted.

temperature dependences of the T_1 above and below the T_g were shown by Sato et al. using long-pulse saturation recovery technique.[7] On the other hand, to estimate the effect of the T_2, three spin-labeled PCHA's having different nitroxide concentrations, PCHA-1, PCHA-2, and PCHA-3, were prepared by the blending with nonlabeled PCHA (Table 1). A decrease in the T_2 is expected with an increase in the nitroxide concentration. However, the nitroxide concentration little affected on the temperature dependence of the S_{121mW} (see Supporting Information). From these results, it is concluded that the nitroxide concentrations of the samples are low enough and the effect of the T_2 is ignored; therefore, the inflection in the temperature dependence of the S_{121mW} is due to the difference in the temperature dependence of the T_1 in the glassy and rubbery states of the PCHA. The inflection point in the temperature dependence of the S_{121mW} was defined as $T_{g,\ ESR}$. To verify the experimental uncertainty on the $T_{g,\ ESR}$, the measurements were separately carried out four times for the PCHA-1; the $T_{g,\ ESR}$ values were 286, 286, 287, and 289 K, respectively (Table 1). Therefore, the average $T_{g,\ ESR}$ of the spin-labeled PCHA is 287 K, and the experimental uncertainty is better than ± 2 K. It should be noted that the T_g generally depends on the cooling rates; therefore, there is small ambiguity for comparing the $T_{g,\ ESR}$ with the $T_{g,\ DSC}$ since different cooling rates are used for the DSC and the ESR. However, Santangelo and Roland showed that the $T_{g,\ DSC}$ measured at the cooling rate of 10 K min^{-1} was in good agreement with the dilatometric T_g measured with the stepwise temperature change as well as the present ESR method.[16] Therefore, the $T_{g,\ DSC}$ measured at the cooling rate of 10 K min^{-1} was compared to the $T_{g,\ ESR}$ in this work.

In the Supporting Information, the temperature dependences of S's measured at the P of 49, 81, 121, and 169 mW are compared. The S increased with an increase in the P. On the other hand, the $T_{g,\ ESR}$ values determined from the temperature dependences of these S's agreed within 1 K. This result shows that the increase in the local temperature around the nitroxides by the irradiation of the high power microwave is negligible.

B. Glass Transition Temperature of PCHA around Chain Ends. A T_g of a polymer generally decreases with a decrease in the molecular weight.[17] The reduction of the T_g is proportional to an increase in the chain end concentration. Therefore, it is suggested that polymer chain ends have high mobility with large free volume and they depress the T_g. In fact, the large free volume around chain ends was demonstrated by the photolabel method.[18,19] Moreover, an increase in the free volume fraction with increasing the chain end concentration was shown by the positron annihilation lifetime measurement[20] and the dilatometric measurement.[21]

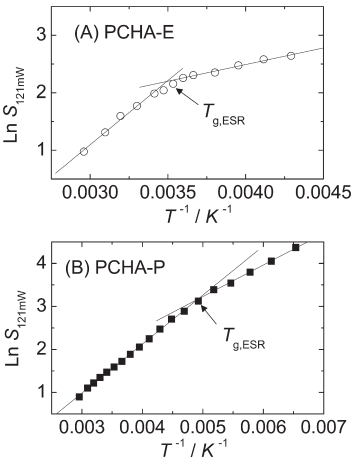

Figure 4. Temperature dependence of S_{121mW} for PCHA-E (A) and PCHA-P (B). The data points are least-squares fitted.

These results also show that chain ends have large free volume. Previously, we compared the mobility of chain ends and midchain segments for several polymers using the site specific spin-label method.[10,12,22] In the previous works, $T_{5.0mT}$ at which the motional correlation time, τ_c, is equal to ca.10 ns was determined as a reference temperature. The $T_{5.0mT}$ was about 70 K higher than the $T_{g,\ DSC}$. The $T_{5.0mT}$'s of end-labeled polymers were lower than those of midchain-labeled polymers, which indicates the higher mobility of chain ends.

In the present work, the difference between local T_g around chain ends and that around midchains is determined using the PCHA-E and PCHA-1 which are labeled with the same nitroxides, but only the label positions are different. The PCHA-E has almost the same M_n with the PCHA-1 (Table 1). Temperature dependence of the S_{121mW} for the PCHA-E is shown in Figure 4A. The $T_{g,\ ESR}$ of the PCHA-E was separately determined three times and the values were 283, 284, and 286 K, respectively. The average of these values is 284 K and the experimental uncertainty is better than ± 2 K. As described above, the average $T_{g,\ ESR}$ of the PCHA-1 which is spin-labeled midchain segments is 287 K ± 2 K. Therefore, this result demonstrates that the $T_{g,\ ESR}$ around chain ends is about 3 K lower than that around midchain segments because of the higher mobility around chain ends. Nevertheless, one may expect much larger difference in the mobilities of chain ends and midchain segments. Certainly, much higher local mobility of chain ends compared to that of midchain segments was shown for polystyrene in diluted solution by the fluorescence depolarization method.[23] However, in the bulk state, polymer segments move cooperatively with neighboring segments; the length scale of the cooperativities is reported to be a few nm around the glass transition.[24,25] In this situation, chain end segments must move cooperatively with neighboring midchain segments. Hence, the reduction of T_g around chain ends was not remarkable.

C. Detection of $T_{g,\ ESR}$ by Spin-Probe Method. The temperature dependence of the S_{121mW} for the PCHA-P in which small amount of TEMPOL is dispersed as spin-probes is shown in Figure 4B. The PCHA-P showed an inflection in the temperature dependence of the S_{121mW} at 203 K. This value is much lower than the $T_{g,\ DSC}$, 286 K. This result shows that the molecular tumbling motion of the TEMPOL is decoupled with the glass transition of the PCHA. Sillescu studied the size dependence of the diffusion coefficient of low molecular weight probes in supercooled liquids.[26] As the size of probes was larger than the solvent molecules, the probe

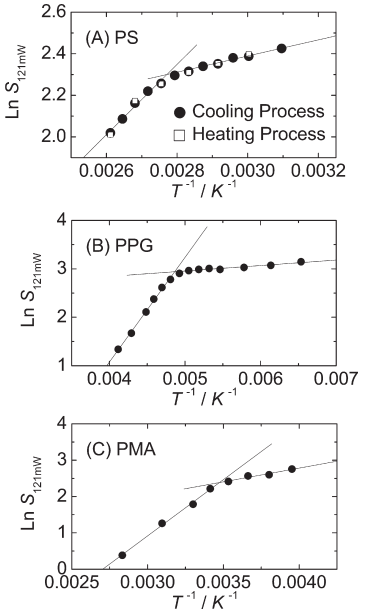

Figure 5. Temperature dependence of S_{121mW} for PS (A), PPG (B), and PMA (C). The data points are least-squares fitted. The open symbol is the S_{121mW} determined in the heating process.

diffusion was coupled to the shear viscosity of the solvent. On the other hand, when the probe size was smaller than the solvent size, the probe diffusion coefficient increased with the decrease in the probe size. Therefore, it is concluded that the size of the TEMPOL is small to be coupled with the segmental motion of the PCHA at the glass transition.

D. Measurement of $T_{g,\ ESR}$ for Various Amorphous Polymers. Temperature dependences of S_{121mW} for spin-labeled PS, PPG, and PMA are shown in Figure 5, parts A−C, respectively. These polymers showed an inflection in the temperature dependence of the S_{121mW}. The $T_{g,\ ESR}$'s of the PS, PPG, and PMA were determined to be 360, 285, and 204 K, respectively. These values are in good with $T_{g,\ DSC}$'s within experimental uncertainties (Table 1). This result demonstrates that this ESR technique can be widely applied for various polymers.

The S_{121mW} determined in the heating process is compared to that determined in the cooling process for the PS in Figure 5A. These values agreed well with each other. Therefore, it is verified that both the heating process and cooling process provide the corresponding $T_{g,\ ESR}$ values because the microwave power saturation measurement is carried out with the stepwise temperature variation.

E. Determination of T_g in Highly Crystallized PEG. The ESR technique was applied to determine the T_g in highly crystallized PEG while the DSC could not detect the glass transition. The DSC trace of PEG is shown in Figure 6A. A distinct melting transition is observed at 338 K and the degree of crystallinity is calculated at 91%, using 222.2 J/g as the fusion enthalpy of PEG crystallites.[27] On the other hand, no glass transition was detected because of the high crystallinity. Although Vaia et al. detected very small glass transition of poly(ethylene oxide) (PEO) by the DSC scanned with very high heating rate, 40 K/min, the detection of the glass transition in highly crystallized PEG and PEO is very hard.[28] Thermally stimulated current (TSC) is much sensitive than the DSC; therefore, the T_g of the PEO was determined to be 218 K.[28]

For the PEG, the temperature dependence of the S_{121mW} was measured in the heating process. The temperature dependence of the S_{121mW} for the PEG is shown in Figure 6B, and the $T_{g,\ ESR}$ is determined to be 221 K. This value is in agreement with the T_g determined by the TSC, 218 K.[28] In the PEG, the labeled nitroxides are excluded from the crystallites and only exist in the amorphous region. Therefore, the molecular tumbling motion of the spin-labels is affected by the glass transition of the amorphous region. This result shows that the ESR technique is useful to determine the T_g even for highly crystallized polymers.

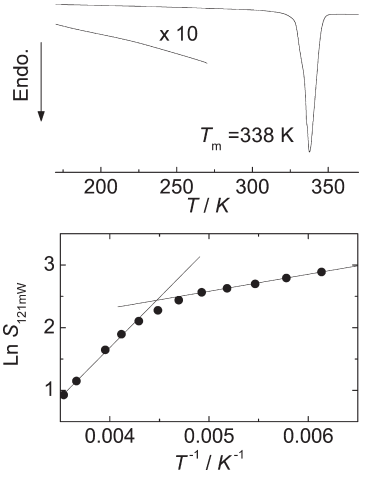

Figure 6. DSC trace (A) and temperature dependence of S_{121mW} (B) for PEG. The data points are least-squares fitted.

Conclusion

The $T_{g,\ ESR}$ was determined from the temperature dependence of the saturation factor, S, for spin-labeled polymers. The $T_{g,\ ESR}$'s was in good agreement with the $T_{g,\ DSC}$ for the PCHA, PS, PMA, and PPG. Furthermore, results have shown that the local T_g around chain ends is somewhat lower than that around midchain segments for the PCHA. Finally, the $T_{g,\ ESR}$ for highly crystallized PEG was determined while the $T_{g,\ DSC}$ was unable to be determined. As a conclusion, a novel and effective ESR application to determine T_g's at local sites of polymeric materials has been developed.

Acknowledgment. The author expresses his sincere thanks to Professor Shulamith Schlick of University of Detroit Mercy for commenting on the draft of this paper. The author also thanks Dr. Katsuhiro Yamamoto for supplying the spin-labeled polymers and Professor Shigetaka Shimada for his fruitful discussion.

Supporting Information Available: Figure S-1, presenting the comparison of the temperature dependences of S_{121mW} for the PCHA-1, PCHA-2, and PCHA-3, and temperature dependences of S_{49mW}, S_{81mW}, S_{121mW}, and S_{169mW} for the PCHA-2, shown in Figure S-2. This material is available free of charge via the Internet at http://pubs.acs.org.

References and Notes

(1) Strobl, G. R. *The Physics of Polymers*; Springer: Berlin, 1996; pp 237−256.
(2) Sanchez, I., Ed. *Physics of Polymer Surfaces and Interfaces*, Butterworth-Heinemann: Boston, MA, 1992; pp 1−262.
(3) Ellison, C. J.; Torkelson, J. M. *Nat. Mater.* **2003**, *2*, 695.
(4) Earle, K. A.; Budil, D. E. In Schlick, S., Ed., *Advanced ESR Methods in Polymer Research*; Wiley: Hoboken, NJ, 2006; Chapter 3, pp 53−83.
(5) Jeschke, G.; Schlick, S. In *Advanced ESR Methods in Polymer Research*; Schlick, S., Ed.; Wiley: Hoboken, NJ, 2006; Chapter 1, pp 3−24.
(6) Andreozzi, L.; Giordano, M.; Leporini, D.; Martinelli, M.; Pardi, L. *Phys. Lett. A* **1991**, *160*, 309.

(7) Sato, H.; Bottle, S. E.; Blinco, J. P.; Micallef, A. S.; Eaton, G. R.; Eaton, S. S.; et al. *J. Magn. Reson.* **2008**, *191*, 66.
(8) Spielberg, J. I.; Gelerinter, E. *Phys. Rev. B* **1984**, *30*, 2319.
(9) Spielberg, J. I.; Gelerinter, E. *Phys. Rev. A* **1985**, *32*, 3647.
(10) Miwa, Y.; Tanase, T.; Yamamoto, K.; Sakaguchi, M.; Sakai, M.; Shimada, S. *Macromolecules* **2003**, *36*, 3235.
(11) Miwa, Y.; Yamamoto, K.; Sakaguchi, M.; Sakai, M.; Tanida, K.; Hara, S.; Okamoto, S; Shimada, S. *Macromolecules* **2004**, *37*, 831.
(12) Miwa, Y.; Tanabe, T.; Yamamoto, K.; Sugino, Y.; Sakaguchi, M.; Sakai, M.; Shimada, S. *Macromolecules* **2004**, *37*, 8612.
(13) Miwa, Y.; Drews, A. R.; Schlick, S. *Macromolecules* **2008**, *41*, 4701.
(14) Brezina, G. W.; Gelerinter, E. *J. Chem. Phys.* **1968**, *49*, 3293.
(15) Robinson, B. H.; Haas, D. A.; Mailer, C. *Science* **1994**, *263*, 490.
(16) Santangelo, P. G.; Roland, C. M. *Macromolecules* **1998**, *31*, 4581.
(17) Fox, T. G.; Flory, P. J. *J. Appl. Phys.* **1950**, *21*, 581.
(18) Yu, W.; Sung, C. S. P.; Robertson, R. E. *Macromolecules* **1988**, *21*, 355.
(19) Yu, W.; Sung, C. S. P. *Macromolecules* **1988**, *21*, 365.
(20) Li, H.; Ujihira, Y.; Nanasawa, A. *Kobunshi Ronbunshu* **1996**, *53*, 358.
(21) Richardson, M. J.; Savill, N. G. *Polymer* **1977**, *18*, 3.
(22) Miwa, Y.; Yamamoto, K.; Sakaguchi, M.; Sakai, M.; Makita, S.; Shimada, S. *Macromolecules* **2005**, *38*, 832.
(23) Horinaka, J.; Maruta, M.; Ito, S.; Yamamoto, M. *Macromolecules* **1999**, *32*, 1134.
(24) Adam, G.; Gibbs, J. H. *J. Chem. Phys.* **1965**, *43*, 139.
(25) Rizos, A. K.; Ngai, K. L. *Phys. Rev. E* **1999**, *59*, 612.
(26) Heuberger, G.; Sillescu, H. *J. Phys. Chem.* **1996**, *100*, 15255.
(27) Braun, W.; Hellwege, K.-H.; Knappe, W. *Kolloid-Z. Z. Polym.* **1967**, *215*, 10.
(28) Vaia, R. A.; Sauer, B. B.; Tse, O. K.; Giannelis, E. P. *J. Polym. Sci., Part B: Polym. Phys.* **1997**, *35*, 59.